33rd Annual International Conference of the IEEE EMBS
Boston, Massachusetts USA, August 30 - September 3, 2011

Temporal Segmentation of Lung Region from MRI Sequences Using Multiple Active Contours

Renato Seiji Tavares, José Miguel Manzanares Chirinos,
Leonardo Ishida Abe, Toshiyuki Gotoh, Seiichiro Kagei
Tae Iwasawa and Marcos de Sales Guerra Tsuzuki

Abstract— **Segmentation of the lung is particularly difficult because of the large variation in image quality. A modified Hough transform in combination with a mask creation algorithm can robustly determine synchronous respiratory patterns. The synchronicity restriction is relaxed by applying a greedy active contour algorithm. The respiratory patterns define a point cloud near the lung region boundary representing a subjective contour. The gravitation vector field (GVF) active contour algorithm is used to create an initial segmentation exclusively based on the point cloud. A final active contours algorithm is executed to adjust the boundary to the images. The algorithm was tested with healthy subjects and COPD patients, and the result was checked through temporal registration of coronal and sagittal images.**

I. INTRODUCTION

Segmenting the lungs in medical images is a challenging and important task for many applications. Several methods have been proposed for the segmentation of lungs from Computed Tomography (CT) images. Most algorithms use grey level thresholding followed by active contour segmentation [1]. Previous work have shown that MR images cannot be segmented as accurately as CT images [2].

The work presented here is part of a larger effort to develop automated 3D animated lung reconstruction [3]. This way, segmentation is an intermediate step in the registration and 3D reconstruction. Our MR images cannot be handled exclusively with the intensity of the gradients. Intensities vary non uniformly throughout a single structure and the boundary between neighboring structures may be noisy. The lung boundaries can either poorly defined or obscured by surrounding tissues with almost similar grey levels.

This work is structured as follows. Section II explains the temporal lung segmentation where a greedy active contour algorithm is applied to relax the synchronicity restriction. Section III explains how the lung region boundary is extracted using two active contours algorithms. In section IV, more results are presented. Finally, section V rounds up the paper with the conclusions.

This work is supported by FAPESP (Grant 2010/19685-5) and CNPq (Grant 471.119/2010-5).

RS Tavares is supported by FAPESP (Grant 2010/18658-4), JMM Chirinos is supported by CNPq (Grant 506.866/2010-6) and MSG Tsuzuki was partially supported by CNPq (Grants 304.258/2007–5 and 309.570/2010–7). RS Tavares, JMM Chirinos, LI Abe and MSG Tsuzuki are with Computational Geometry Laboratory, Escola Politécnica, São Paulo University, Brazil. mtsuzuki@usp.br.

T Gotoh and S Kagei are with Yokohama National University, Japan.

T Iwasawa is with Kanagawa Cardiovascular and Respiratory Center, Japan.

II. TEMPORAL LUNG SEGMENTATION

Tavares et al. [4] proposed an algorithm to realize the temporal segmentation of the lung. It is based on a spatio temporal volume (STV) defined by stacking images from temporal sequences. This method is based on the assumption that lungs related structures do move almost synchronously, and synchronous respiratory patterns were determined in two dimensional spatio temporal (2DST) images by a modified Hough transform [5], [6], [7], [8].

The modified Hough transform determines the presence of respiratory patterns through a voting procedure. This method does not allow the automatic determination of which lung structures or boundaries are associated with the found respiratory patterns. In our specific case, we are interest in determining the respiratory patterns associated with the diaphragmatic and apex surfaces.

The method proposed by Tavares et al. [4] controls the modified Hough transform through a mask that approximates the lung region boundary. The mask creation algorithm is not robust, and some masks can be totally wrong. However, the combination of 2DST masks and modified Hough transform showed to be very robust.

A. Determining Asynchronous Respiratory Patterns

It is known that the lung related structures do not move synchronously. Consequently, the respiratory patterns found by the modified Hough transform do not correspond to real movement and they must be relaxed. The respiratory patterns are processed by a greedy active contour algorithm [9] that adjusts asynchronous discrepancies.

The respiratory pattern that resulted from the modified Hough transform is the initial condition for the greedy active contour algorithm. A respiratory pattern $f_k(t)$ is a set of pixels with only one pixel for every vertical line (see Fig. 1). It is given by

$$f_k(t) \Longleftrightarrow \{y_0, y_1, \cdots, y_n\}$$

where $0 \leq t \leq n$ and n is the number of frames. The energy function to be minimized is defined as

$$E(f_k(t)) = E_{int}(f_k(t)) + E_{image}(f_k(t))$$

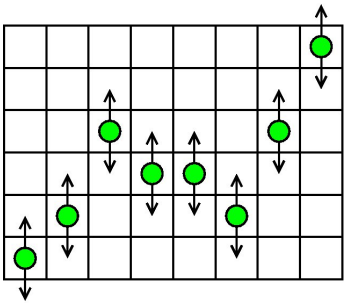

Fig. 1: A respiratory pattern determined by the modified Hough transform. The active contour algorithm searches in the vertical adjacency of the pixels belonging to the respiratory pattern, for a position with smaller energy.

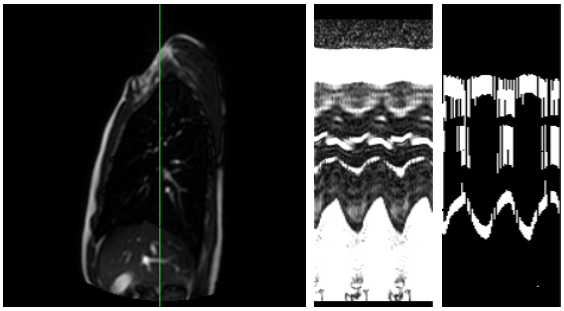

(a) (b) (c)

Fig. 2: (a) A sagittal image showing where a 2DST image has been taken. (b) A 2DST image. (c) A 2DST mask with two main respiratory patterns.

where E_{int} is the internal energy and it is defined by

$$E_{int}(f_k(t)) = \frac{1}{2}\sum_{t=0}^{t=n}\left(\alpha \cdot |\frac{\partial f_k(t)}{\partial t}|^2 + \beta \cdot |\frac{\partial^2 f_k(t)}{\partial t^2}|^2\right) \quad (1)$$

where α and β are positive parameters. E_{image} is the term that pulls the respiratory pattern to the pixels with higher intensity in the edge image. The edge image is obtained by applying a gradient filter to the original image. It is defined by

$$E_{image}(f_k(t)) = -\frac{\gamma}{\sigma(I(f_k(t)))} \cdot \mu(\nabla I(f_k(t))) \quad (2)$$

where γ is a positive parameter, $\sigma(I(f_k(t)))$ is the standard deviation of the intensity of pixels composing the respiratory pattern (original image) and $\mu(\nabla I(f_k(t)))$ is the respiratory pattern edge pixels intensity average (edge image).

B. Greedy Active Contour and Masks Creation

Tavares et al. [4] included black masks in the 2DST mask when incorrect masks were created. This decision showed to be reasonable with the modified Hough transform, even considering that black masks transferred no image information to the process. In this work, we used completely white lines instead, improving the result of the active contours algorithm as more information about the image is present.

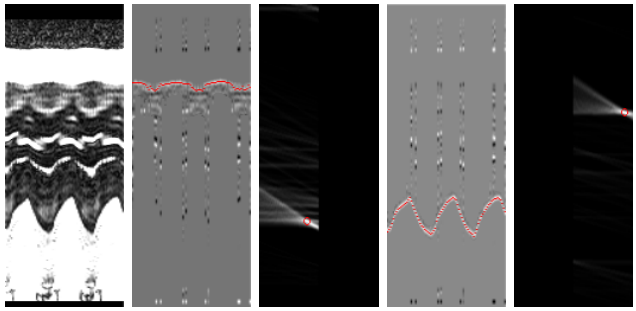

(a) (b) (c) (d) (e)

Fig. 3: Temporal processing using the modified hough transform. (a) A vertical 2DST image. (b) The edge image obtained with the mask applied for the superior surface contour. (c) The Hough space showing the detected respiratory pattern in (b). (d) The edge image obtained with the mask applied for the inferior surface contour. (e) The Hough space showing the detected respiratory pattern in (d).

A 2DST mask is shown in Fig. 2. Two main respiratory pattern regions are present, relative to the apex surface and the diaphragmatic surface. Other white regions in image come from invalid masks and they will be substituted by completely white verticals. Fig. 3(a) shows a vertical 2DST image with high intensity pixels, representing fat or blood vessels, filtered. The intersection of the 2DST with the mask results in two edge images. Fig. 3(b) and (d) show the edge images for the upper (appex) and lower (diaphragmatic) respiratory pattern regions, respectively. Fig. 3(c) and (e) respectively show the Hough spaces for the upper and lower respiratory pattern regions. The pixel with highest intensity in each Hough space is detected, and it represents a respiratory pattern shown in the respective edge image after the greedy active contour processing, Fig. 3(b) and (d). This method is applied on four directions: vertical, horizontal and both diagonals. The result is shown in Fig. 4, in which colors indicate which processing direction detected that given pattern.

III. Contour Extraction

Fig. 4 represents a subjective contour, in the shape of the lung silhouette.The active contours algorithm should be used to extract a contour from such point cloud. However, as most implementations rely on an edge map as the main external force, the initial contour is of extreme importance for the quality and correctness of the final result. Considering that at this stage an adequate initial contour is not available, the gravitational vector field (GVF) active contours is used instead [10].

A. Contour extraction using GVF active contours

Fig. 5(a) shows the same point cloud displayed in Fig. 4, but as white pixels in a binary image. Using GVF active contours, a random initial contour can be used, and the initial contour used is shown in Fig. 5(b). The GVF field created

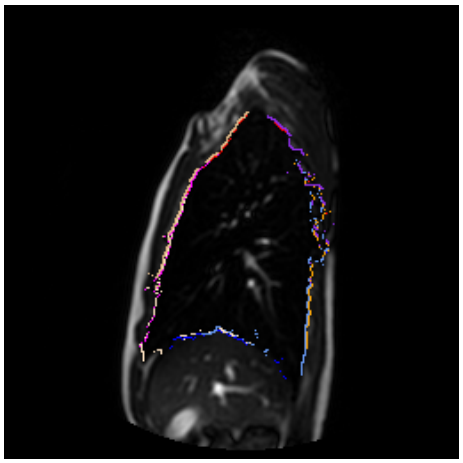

Fig. 4: Subjective contour represented by a cloud of points resulted from the temporal processing.

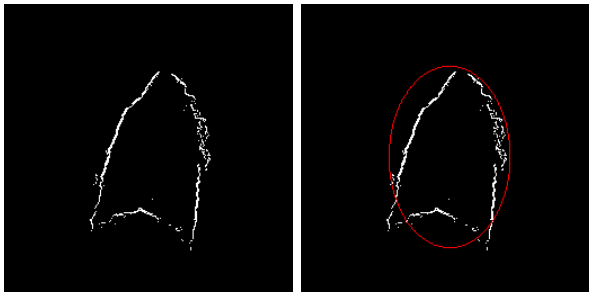

(a) (b)

Fig. 5: (a) Point cloud detected by the temporal segmentation. (b) Random initial contour.

for this image is shown in Fig. 6(a). It can be seen that instead of an edge map with large gradients restricted to the surrounding edges, a large dense region of force vectors is created. Two small sections of the image are selected and closer shown in Fig. 6(b) and (c). Fig. 6(b) was taken around the image bottom left corner of the lung, whereas Fig. 6(c) was taken around the spine, on the right. In both images, the force field vectors can be seen more easily.

In Fig. 6(b), it can be seen that the force vectors point towards the obtained point cloud, resulting in the contour being attracted to these points. However, one can notice a lack of points for a more precise contour convergence. In particular, there is a tendency for the points in the leftmost bottom corner to be cut out from the final contour, as there is only a line of points in the left bottom over which the contour slides to a position where it is smoother. This lack of points from the temporal segmentation can be corrected by using the image itself, through a final adjusting step with a traditional active contours algorithm.

In Fig. 6(c), on the other hand, there is an excess of points. This is a region of low contrast, and as a result the temporal segmentation obtains a large set of points that do not precisely define a contour. In this case, the active

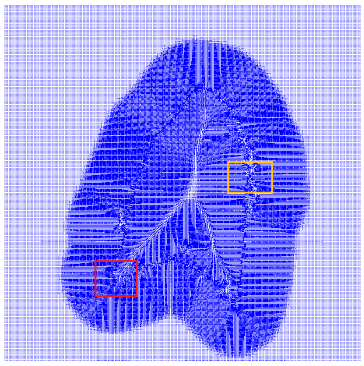

(a)

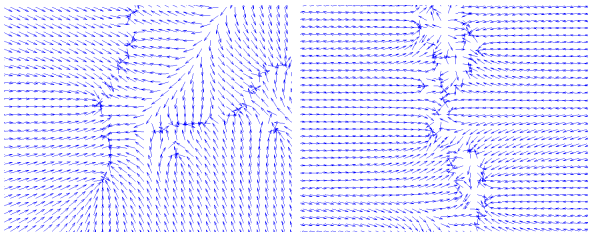

(b) (c)

Fig. 6: GVF field obtained by processing the point cloud from Fig. 5(a). (a) Details from the Lung bottom left corner. (b) Details from the Spine region.

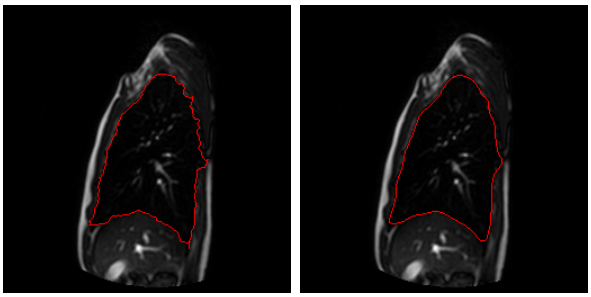

(a) (b)

Fig. 7: (a) Extracted contour compared to base image. (b) Compared to points obtained from temporal processing.

contours algorithm obtains a contour that necessarily skips most of those points. This contour can be refined using the original image also.

Fig. 7(a) shows the result of the GVF active contours algorithm. This contour, however, does not approximate the lung region boundary, but the point cloud obtained by the temporal segmentation. It is not smooth and may be wrongly positioned at certain regions, due to the lack or excess of points. A traditional active contours algorithm is used to correct the boundary. However, in this stage, an initial contour close to the desired contour is available as a result from the GVF active contours algorithm. The result of this final step is shown in Fig. 7(b). It can be seen that both corners were accurately extracted.

IV. Results

The temporal segmentation has difficulties in the lung bottom corners in images at the inspiration phase of the breathing cycle, mostly due to the concave shape of the diaphragm. At a given time instant, the diaphragm may be present in a diagonal 2DST image, but moments later, the diaphragm does not intersect the 2DST. The respiratory pattern for this 2DST has no meaning at all. If no 2DST can provide a valid respiratory pattern, there will be a lack of points for the contour extraction algorithm, causing over smoothing of the corners.

Fig. 8 shows the extracted contours for a temporal sagittal sequence. Fig. 8(b) compares the extracted contours shown in Fig. 8(a) with the temporal processing points. In both cases, the corners are sharp, and the most difficulty region was the spine, due to the local low image contrast. Fig. 8 (e) and (f) shows the contours extracted for two images in a temporal coronal sequence. The bottom corners seem sharp enough, and the contour is smooth. The region near the heart was not segmented accurately enough, though, but to delineate the lung boundary in such region is difficulty, due to the proximity of the heart, important blood vessels and lung internal structures.

The proposed algorithm was applied to sagittal and coronal MR image sequences and the position of the diaphragmatic and apex surfaces were determined at the intersecting vertical segment. By analyzing the extracted lung region boundary a temporal registration was executed (see Fig. 9) and the coherence of the images was checked.

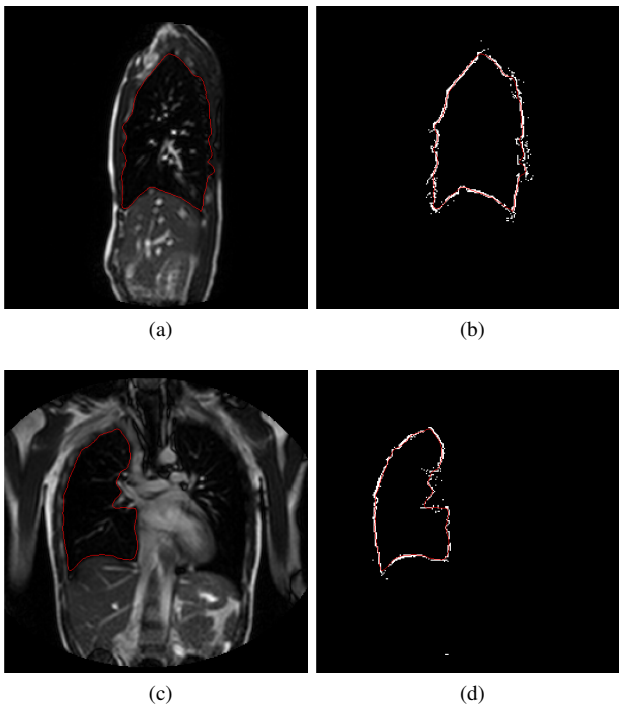

(a) (b) (c) (d)

Fig. 8: (a)-(c) Extracted contour compared to base image. (b)-(d) Compared to point cloud obtained from improved temporal segmentation.

V. Conclusions and Future Works

In this work, the temporal segmentation algorithm by Tavares et al. [4] was improved, creating point cloud more precise, and a valid contour is extracted using GVF and conventional active contours algorithms applied in sequence. The valid contours are smooth, and lung corners are sharp enough for most images. Results could be improved with the use of more optimal MR sequences/protocols. Still, the proposed method is able to obtain valid contours for all images in a temporal series, even in images with poor quality and low contrast.

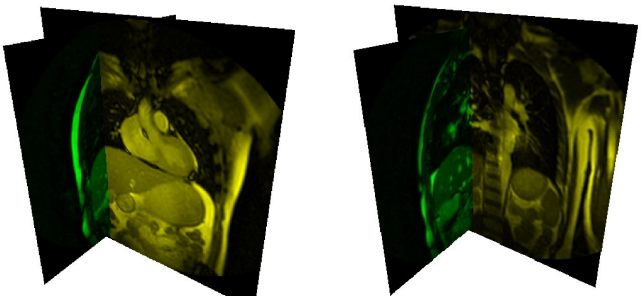

(a) (b)

Fig. 9: (a)-(b) 3D compositions of one coronal and one sagittal images.

References

[1] M. Silveria and J. Marques, "Automatic segmentation of the lungs using multiple active contours and outlier model," in *Proc 28nd Annu Int Conf IEEE EMBS*, New York, USA, 2006, pp. 3122–3125.

[2] L.P. Clarke, R.P. Velthijizen, M.A. Camacho, J.J. Heine, M. Vaidyanathan, L.O. Hal, R.W. Thatcher, and M.L. Silbiger, "MRI segmentation: Methods and applications," *Magnetic Resonance Imaging*, vol. 13, pp. 343–368, 1995.

[3] M.S.G. Tsuzuki, F.K. Takase, T. Gotoh, S. Kagei, A. Asakura, T. Iwasawa, and T. Inoue, "Animated solid model of the lung constructed from unsynchronized mr sequential images," *Computer Aided Design*, vol. 41, pp. 573–585, 2009.

[4] R.S. Tavares, A.K. Sato, M.S.G. Tsuzuki, T. Gotoh, S. Kagei, A. Asakura, and T. Iwasawa, "Temporal segmentation of lung region MR images sequences using hough transform," in *Proc 32nd Annu Int Conf IEEE EMBS*, Buenos Aires, Argentina, 2010, pp. 4789–4792.

[5] A. Asakura, T. Gotoh, S. Kagei, T. Iwasawa, and T. Inoue, "Computer aided system for respiratory motion analysis of the lung region by sequential MR images," *Med Imag Techn*, vol. 23, pp. 39–46, 2005.

[6] K. Matsushita, A. Asakura, S. Kagei, T. Gotoh, T. Iwasawa, and T. Inoue, "Shape tracking on chest MR sequence images using respiratory patterns," *JIIEEJ*, no. 33, pp. 1115–1122, 2004.

[7] R.S. Tavares, M.S.G. Tsuzuki, T. Gotoh, S. Kagei, and T. Iwasawa, "Lung movement determination in temporal sequences of MR images using Hough transform and interval arithmetics," in *Proc 7th IFAC Symp MCBMS*, Aalborg, Denmark, 2009, pp. 192–197.

[8] A.K. Sato, N. Stevo, R.S. Tavares, M.S.G. Tsuzuki, E. Kadota, T. Gotoh, S. Kagei, A. Asakura, and T. Iwasawa, "Registration of temporal sequences of coronal and sagittal MR images through respiratory patterns," *Biomed Signal Process Control*, vol. 6, pp. 34–47, 2011.

[9] D.J. Williams and M. Shah, "A fast algorithm for active contours and curvature estimation," *CVGIP: Image Underst*, vol. 55, pp. 14–26, 1992.

[10] C. Xu and J. Prince, "Snakes, shapes, and gradient vector flow," *IEEE Transactions on Image Processing*, vol. 7, no. 3, pp. 359–369, 1998.